R-matrix calculation of low-energy electron collisions with uracil

Amar Dora,[1] Jonathan Tennyson,[1,a)] Lilianna Bryjko,[2] and Tanja van Mourik[2]
[1]*Department of Physics and Astronomy, University College London, Gower Street, London WC1E 6BT, United Kingdom*
[2]*School of Chemistry, University of St. Andrews, North Haugh, St. Andrews, Fife KY16 9ST, United Kingdom*

(Received 10 January 2009; accepted 26 March 2009; published online 24 April 2009)

R-matrix calculations on electron-uracil collisions are presented within the static exchange, static exchange plus polarization, and close-coupling approximations. Particularly as input for the close-coupling calculations, a series of target calculations is performed which considers low-lying singlet and triplet excited states of the uracil target. The scattering calculations find three low-lying shape resonances of $^2A''$ symmetry and three higher-energy Feshbach resonances of $^2A'$ symmetry. In both symmetries the precise resonance parameters are found to be sensitive to the treatment of polarization effects employed. Cross sections are presented for both elastic scattering and electronic excitation. Comparisons are made with energy-dependent, differential cross section measurements at 90° angle and good agreement is found for scattering energies above 0.5 eV. © *2009 American Institute of Physics*. [DOI: 10.1063/1.3119667]

I. INTRODUCTION

Since the pioneering work on the effect of low-energy electrons on strand breaks in DNA by Boudaïffa *et al.*,[1] there has been extensive investigation of electron collisions with the various constituents of DNA because of the potential importance of this process for radiobiology.[2] For this uracil has become something of a benchmark system and, particularly since the work of Boudaïffa *et al.*, increasingly many experimental[3–13] and theoretical[14–19] studies focusing on aspects of low-energy electron collisions, as well as studies of weakly bound anion states, have appeared in the literature.[20,21] A particular focus of interest has been the characterization of low-lying resonance states where the electron temporarily attaches to the uracil; such resonances are thought to be the route to strand breaks in DNA.

Resonance states are often characterized as shape resonances, where the scattering electron temporarily occupies a low-lying unoccupied target orbital and Feshbach or core-excited resonances that involve simultaneous excitation of the target. Most previous theoretical work has concentrated on shape resonances which can generally be characterized using relatively straightforward models. See the *R*-matrix calculations by Tonzani and Greene for example.[17] More demanding calculations are required to characterize Feshbach resonances and it can be harder to obtain definitive parameters for these resonances. Thus the most sophisticated collision studies which are due to Winstead and McKoy[18,22–24] found evidence for Feshbach resonances in the electron-uracil problem but did not characterize them.[18]

In this paper we present a series of calculations on the electron-uracil problem. The aim of these studies is to develop stable and reliable models for characterizing the resonances, both shape and Feshbach, in uracil and to compute the associated collision cross sections. Our aim is to develop predictive models that can be applied to electron collisions with other small biomolecules without repeating the extensive series of tests reported here. Such testing is necessary since previous *R*-matrix calculations on electron collisions with tetrahydrofuran[25] missed the shape resonances in this system.[26,27] This problem appears to be associated with the inclusion of too few virtual orbitals in the calculation. Similar problems were found with some of our initial models in the present work.

II. THEORY

Computational implementations of the *R*-matrix method are based on different formulations of the problem;[28,29] the method employed here is based on the division of space into an internal region containing all the *N*-electron target charge cloud and an external scattering region. In the inner region the discretized continuum $(N+1)$-electron wave function ψ_k^{N+1} is written in the form of a close-coupling (CC) expansion

$$\psi_k^{N+1} = \mathcal{A}\sum_{ij} a_{ijk}\Phi_i(\mathbf{x}_1, \ldots, \mathbf{x}_N)u_{ij}(\mathbf{x}_{N+1}) + \sum_i b_{ik}\chi_i(\mathbf{x}_1, \ldots, \mathbf{x}_{N+1}), \quad (1)$$

where Φ_i represents a target state and u_{ij} represents extra orbitals introduced to represent the scattering electron. These are antisymmetrized by operator $\mathcal{A}$. The second summation in Eq. (1) involves L^2 configurations where all electrons are placed in orbitals associated with the target. Such configurations are essential in even the simplest model which does not include any target relaxation, the static exchange (SE) approximation, to allow for orthogonalization between the continuum orbitals and those belonging to the target. In more sophisticated models L^2 configurations are also essential for

a)Electronic mail: j.tennyson@ucl.ac.uk.

 © 2009 American Institute of Physics

Downloaded 30 Apr 2009 to 128.40.5.98. Redistribution subject to AIP license or copyright; see http://jcp.aip.org/jcp/copyright.jsp

TABLE I. The CASSCF $X\ ^1A'$ ground state energy (in hartree), vertical excitation energies (in eV), and ground state dipole moment (in D) as a function of basis set. The (14, 10) active space was used.

State	6-31G	6-31G*	cc-pVDZ	aug-cc-pVDZ	TZV(2*d*,*p*)	cc-pVTZ
$X\ ^1A'$	−412.350 99	−412.524 43	−412.563 49	−412.585 09	−412.665 57	−412.673 907
$2\ ^1A'$	6.61	6.66	6.59	6.46	6.50	6.54
$3\ ^1A'$	6.96	7.06	7.00	6.94	6.95	6.98
$4\ ^1A'$	8.63	8.74	8.77	8.62	8.65	8.72
$1\ ^1A''$	4.69	4.93	4.92	4.92	4.92	4.93
$2\ ^1A''$	6.17	6.49	6.49	6.47	6.48	6.50
$3\ ^1A''$	7.73	7.92	7.89	7.87	7.87	7.89
$4\ ^1A''$	7.88	8.03	7.96	7.90	7.93	7.93
$1\ ^3A'$	3.79	3.87	3.87	3.84	3.84	3.85
$2\ ^3A'$	5.31	5.50	5.49	5.48	5.48	5.50
$3\ ^3A'$	6.04	6.34	6.36	6.34	6.35	6.38
$4\ ^3A'$	7.58	7.73	7.70	7.62	7.65	7.69
$1\ ^3A''$	4.52	4.76	4.75	4.76	4.75	4.76
$2\ ^3A''$	5.97	6.29	6.29	6.28	6.29	6.31
$3\ ^3A''$	7.62	7.82	7.78	7.76	7.76	7.78
$4\ ^3A''$	7.86	8.00	7.93	7.87	7.90	7.91
$\mu(X\ ^1A')$	4.27	4.14	4.06	4.20	4.19	4.15

introducing the effects of target polarization. Given that both shape and Feshbach resonances are localized in the region of the target then it is clear that the resonance parameters will also be sensitive to which of these configurations are included in the calculation.

A particular issue in the choice of both target wave function representation and the L^2 configurations is one of balance. Since, for many-electron targets, neither the target nor the scattering wave functions have energies that are even close to the exact values for the problem, it is the relative energy between the N and $(N+1)$ electron systems that matters. Balancing these two calculations requires a careful choice of configurations; our favored approach is to base models around a complete active space (CAS) valence configuration interaction (CI) representation of the target wave function.[30] Our experience shows that getting a good representation of the target states employed in the CC expansion within this CAS-CI model requires careful choice of orbitals. The implication of previous studies on electron-uracil[18] (and indeed other molecules) is that the choice of orbitals is also important for successfully representing the shape resonances. This is something we test below. The upshot of these issues is that the first step in this study was a series of quantum chemistry calculations performed with the aim of (a) characterizing the low-lying electronic states of uracil and (b) generating a suitable set of orbitals for use in the scattering calculations.

III. CALCULATIONS

A. Target models

The geometry of uracil, optimized with the MP2 method and the 6-31G(*d*) basis set, was taken from Ref. 18; uracil in its equilibrium geometry has C_s symmetry. The 58 electrons of uracil occupy 24σ-orbitals of symmetry A' and 5π-orbitals of symmetry A''. To establish a model methodology to obtain the target orbitals, a series of calculations was performed with the state-averaged complete-active space SCF (SA-CASSCF) method with several basis sets and different active spaces using the MOLPRO 2006.1 computational package.[31] Preliminary results showed that not only the choice of the active space but also the number of calculated states has influence upon the results. In this case 16 states ($4\ ^1A'$, $4\ ^1A''$, $4\ ^3A'$, and $4\ ^3A''$) were calculated. A key problem with CASSCF calculations is scaling with system size: there is a factorial dependence on both the number of active electrons and particularly on the number of active orbitals generating many-electron configurations (full CI within the active space).[32] For atomic or conjugated systems the CAS space typically includes the valence π-orbitals. In heteroatomic systems one may want to include also the lone pair orbitals and electrons to allow for $n \rightarrow \pi^*$ excitations.[33] The full π active space of uracil consists of ten electrons distributed over eight active molecular orbitals (MOs). Including a lone pair MO located on each oxygen yields 14 electrons distributed over ten MOs in the active space. Table I compares the CASSCF $X\ ^1A'$ ground state energy, vertical excitation energies, and ground state dipole moment for the active space consisting of 14 electrons distributed over ten orbitals (14, 10). The calculations were performed with several basis sets: 6-31G, 6-31G*,[34] cc-pVDZ, aug-cc-pVDZ, cc-pVTZ (Refs. 35 and 36), and GAMESS TZV(2*d*,*p*).[37] Even though larger basis sets yield lower ground state energies, the cc-pVDZ basis set gives a dipole moment that is closest to the experimental value of 3.87 D.[38]

Table II compares the CASSCF $X\ ^1A'$ ground state energy, vertical excitation energies, and ground state dipole moment for different active spaces: 12 electrons distributed over nine orbitals (12, 9), 14 electrons distributed over ten orbitals (14, 10), and 14 electrons distributed over 11 orbitals (14, 11). Comparing the results obtained with the (12, 9), (14, 10), and (14, 11) active spaces it is observed that the larger active space leads to the lower value of the ground state energy, and all 15 excited states calculated with the

Downloaded 30 Apr 2009 to 128.40.5.98. Redistribution subject to AIP license or copyright; see http://jcp.aip.org/jcp/copyright.jsp

TABLE II. The CASSCF $X\ ^1A'$ ground state energy (in hartree), vertical excitation energies (in eV), and ground state dipole moment (in D) as a function of active space and basis set.

	(12, 9)		(14, 10)		(14, 11)	
State	6-31G	cc-pVDZ	6-31G	cc-pVDZ	6-31G	cc-pVDZ
$X\ ^1A'$	−412.347 28	−412.559 05	−412.350 985	−412.563 490	−412.361 860	−412.574 134
$2\ ^1A'$	6.68	6.61	6.61	6.59	6.61	6.55
$3\ ^1A'$	7.05	7.13	6.96	7.00	6.95	6.99
$4\ ^1A'$	8.44	8.56	8.63	8.77	8.62	8.76
$1\ ^1A''$	4.42	4.59	4.69	4.92	4.69	4.91
$2\ ^1A''$	7.27	7.34	6.17	6.49	6.18	6.52
$3\ ^1A''$	9.40	9.61	7.73	7.89	7.73	7.89
$4\ ^1A''$	10.42	10.98	7.88	7.96	7.89	7.96
$1\ ^3A'$	3.72	3.79	3.79	3.87	3.79	3.86
$2\ ^3A'$	5.26	5.40	5.31	5.49	5.29	5.48
$3\ ^3A'$	6.16	6.53	6.04	6.36	6.05	6.37
$4\ ^3A'$	7.46	7.55	7.58	7.70	7.56	7.67
$1\ ^3A''$	4.25	4.41	4.52	4.75	4.52	4.74
$2\ ^3A''$	7.18	7.25	5.97	6.29	5.97	6.32
$3\ ^3A''$	9.34	9.54	7.62	7.78	7.63	7.78
$4\ ^3A''$	9.61	9.88	7.86	7.93	7.87	7.93
$\mu(X\ ^1A')$	4.19	3.96	4.27	4.06	4.27	4.07

(14, 10) and (14, 11) active spaces have vertical excitation energies below the ionization potential of uracil, 9.35 ± 0.01 eV.[39] Because the results calculated with the (14, 10) active space differ only slightly from the results calculated with the (14, 11) active space, the (14, 10) active space was chosen to generate the target orbitals for the scattering calculations. CASSCF calculations with the (12, 9) active space using the cc-pVDZ basis set yield a dipole moment that is closest to the experimental value of 3.87.[38] An only slightly higher value of the ground state dipole moment (4.06 D) was received with the (14, 10) active space using the same basis set. We therefore chose the cc-pVDZ basis set for the final calculations.

B. Scattering models

Scattering calculations were performed using the UK molecular *R*-matrix codes.[28] Three basic scattering models were tested. The first model is the SE model in which the target wave function is represented at the Hartree–Fock (HF) level and remains frozen during the collision process. The SE model can only give shape resonances that are usually too high in energy. However the SE model is a well defined approximation which makes the cross comparison between calculations straightforward and meaningful. The second model used is the SE plus polarization (SEP) model in which single excitations out of the target (HF) wave function are used to represent target polarization effects. The SEP model can give good resonance parameters for shape resonances and is also capable of representing Feshbach resonances although this is often more problematic. The final model is the CC model in which several target states are introduced into the first sum in Eq. (1). These states can in principle be represented at the HF level but this usually is not sufficient for electronically excited states so the CAS-CI model is preferred. Here the (14, 10) active space and associated SA-CASSCF orbitals were used. CC calculations are particularly good at representing Feshbach resonances associated with the target excited states explicitly included in the CC expansion. However, even with specially adapted algorithms,[40,41] CC calculations tend to be considerably more computationally expensive than SE or SEP calculations.

Tests concentrated on resonance parameters which, except in a few cases identified below, were obtained automatically using the Breit–Wigner fitting program RESON.[42] Since previous studies identified three shape resonances of $^2A''$ symmetry but no definitive shape resonances with $^2A'$ symmetry, our tests therefore largely concentrated on $^2A''$ symmetry calculations. All studies used Gaussian basis functions with $\ell \leq 4$ (up to *g* orbitals) due to Faure *et al.*[43] located on the center-of-mass and appropriate to the chosen *R*-matrix radius to represent the continuum orbitals. These orbitals were Schmidt orthogonalized to the target orbitals and retained in the calculation, provided that when symmetrically orthogonalized to each other, their eigenvalue was greater than a deletion threshold of 10^{-7}.

Within the SE model there are a limited number of parameters which materially affect the calculation: these are the choice of target basis set used, the number and nature of target virtual orbitals used to give L^2 configurations in Eq. (1) and the *R*-matrix radius. Table III compares the resonance parameters for a selection of our SE calculations with those reported by Winstead and McKoy.[18] The observed positions for the resonances[4,8] are significantly lower and we delay the comparison with these until we consider the SEP and CC models that include polarization effects.

The most notable feature of Table III is the stability of the calculations to changes in the parameters. All studies that used at least 3 a'' virtual orbitals show three resonances in approximately the same positions and the only significant difference is that the SE calculation of Winstead and McKoy[18] found the third resonance to be broader than all our

Downloaded 30 Apr 2009 to 128.40.5.98. Redistribution subject to AIP license or copyright; see http://jcp.aip.org/jcp/copyright.jsp

TABLE III. SE calculations of $^2A''$ symmetry resonance parameters given as position and width in eV as a function of calculation parameters: target basis, R-matrix radius (a in a_0), and number of a'' virtual orbitals retained in the calculation (N_v).

Basis set	a	N_v	Resonance 1	Resonance 2	Resonance 3
6-31G	10	5	2.02, 0.21	4.01, 0.37	8.02, 2.13
6-31G	13	5	2.05, 0.21	4.03, 0.38	8.05, 2.28
cc-pVDZ	13	5	2.26, 0.26	4.44, 0.41	8.57, 2.58
cc-pVDZ	13	10	2.25, 0.26	4.43, 0.41	8.60, 2.70
cc-pVDZ	13	15	2.25, 0.26	4.43, 0.41	8.62, 2.69
cc-pVDZ	13	18	2.25, 0.26	4.42, 0.41	8.63, 2.69
TZV(2d,p)	13	5	2.14, 0.25	4.25, 0.40	8.34, 2.21
TZV(2d,p)	13	5[a]	2.19, 0.25	4.29, 0.41	8.34, 2.51
TZV(2d,p)	13	10	2.14, 0.24	4.25, 0.40	8.27, 2.20
TZV(2d,p)	13	10[a]	2.17, 0.25	4.29, 0.41	8.41, 2.34
TZV(2d,p)	13	15	2.14, 0.24	4.24, 0.41	8.32, 2.31
TZV(2d,p)	13	18	2.13, 0.25	4.24, 0.41	8.32, 2.31
TZV(2d,p)[b]			2.08, 0.23	4.20, 0.44	8.20, 3.00

[a]MVOs generated using a dicationic target.
[b]Reference 18.

SE calculations. Our calculations give similar results for R-matrix radii of 10 and $13a_0$ and show some variation on the target basis set used and little dependence on the number of virtual orbitals retained beyond 3. We tested the use of modified virtual orbitals (MVOs) as recommended by Winstead and McKoy, generating them from HF calculations on cationic uracil. The table shows the results when doubly charged uracil was used (Winstead and McKoy used uracil 4+) which gave resonances with the lowest energies for the MVOs tested. The results were actually marginally worse than calculations using standard HF virtual orbitals.

Although tests were performed at both the SEP and CC level on the R-matrix radius a, we found little sensitivity to choice of a and the calculations reported below are for $a=13a_0$. Table IV compares the resonance parameters for a selection of our SEP calculations. These calculations were all based on a model which kept the lowest 8 a' target core orbitals doubly occupied and allowed holes in the remaining 21 occupied valence orbitals ($9a'-24a'$, $1a''-5a''$). The L^2 configurations associated with this model can be written as

$$(\text{core})^{16}(\text{valence})^{42}(\text{virtual})^{1},$$

$$(\text{core})^{16}(\text{valence})^{41}(\text{virtual})^{2}.$$

In the terminology of second quantization the latter configurations are two-particle-one-hole states. Tests were performed for different choices of target basis functions and as a function of the number of virtual orbitals open for target excitations. The largest of the calculations, which used 18 a' and 18 a'' virtual orbitals, resulted in 13 688 configuration state functions (CSFs). This calculation took about a day on a 64-bit workstation.

TABLE IV. SEP calculations of $^2A''$ symmetry resonance parameters given as position and width in eV as a function of calculation parameters: target basis and number of virtual orbitals retained for each symmetry in the calculation (N_v).

Basis set	N_v	Resonance 1	Resonance 2	Resonance 3
6-31G	5	0.98, 0.06	2.90, 0.24	5.88, 0.77
cc-pVDZ	5	1.29, 0.09	3.39, 0.28	6.48, 0.99
cc-pVDZ	10	0.84, 0.05	2.83, 0.22	5.79, 0.87
cc-pVDZ	15	0.31, 0.015	2.21, 0.16	5.21, 0.72
cc-pVDZ	18	0.072, 0.002	1.94, 0.14	4.97, 0.66
TZV(2d,p)	5	1.35, 0.13	3.38, 0.33	6.94, 1.27
TZV(2d,p)	5[a]	1.05, 0.07	3.25, 0.29	6.26, 0.96
TZV(2d,p)	10	0.91, 0.07	2.91, 0.26	5.92, 0.82
TZV(2d,p)	10[a]	0.54, 0.04	2.76, 0.26	5.66, 0.80
TZV(2d,p)	15	0.44, 0.04	2.26, 0.22	5.41, 0.84
TZV(2d,p)	18	0.174, 0.008	1.96, 0.20	5.08, 0.76
TZV(2d,p)[b]		0.32, 0.018	1.91, 0.16	5.08, 0.40[c]
Obs[d]		0.22	1.58	3.83

[a]MVOs generated using a dicationic target.
[b]Reference 18.
[c]Or 5.06, 0.56 depending on fitting method used (Ref. 18).
[d]Observed (Refs. 4 and 8) resonance positions only.

The resonance parameters obtained from our SEP calculations show some variation with choice of target basis functions (and virtual orbitals) and very considerable variation with respect to the number of virtual orbitals included in the calculation. Indeed the resonance positions drop monotonically as the number of virtual orbitals included in the calculation is increased and show little sign of convergence. This behavior has been seen before in similar calculations on smaller target molecules[44] and is caused by the calculation becoming unbalanced as the correlation of the scattering electron is systematically improved while the target wave function remains uncorrelated. One of the ways to deal with such a situation of unbalanced treatment of correlation is to use the "relaxed-SCF" model for the scattering state as described in Refs. 45 and 46. This model essentially excludes any configurations that involve symmetry breaking of the target ground state. But such a model in our case using 18 virtual MOs of a'' symmetry did not improve the resonance positions very much, giving the position of the lowest $^2A''$ resonance at 1.27 eV.

To try and resolve this problem and at the same time to allow for the electronic excitation and the characterization of

Downloaded 30 Apr 2009 to 128.40.5.98. Redistribution subject to AIP license or copyright; see http://jcp.aip.org/jcp/copyright.jsp

TABLE V. CC calculations of $^2A''$ symmetry resonance parameters given as position and width in eV as a function of calculation parameters: number of target states included (N_s), model as explained in the text and number of virtual orbitals retained for each symmetry in the calculation (N_v). All calculations used the cc-pVDZ target basis and an R-matrix radius of $a=13a_0$.

N_s	Model	N_v	Resonance 1	Resonance 2	Resonance 3
10	A	2	1.60, 0.09	3.69, 0.33	7.72, 2.68
16	A	2	1.35, 0.07	3.37, 0.32	7.47, 2.79
32	A	2	1.14, 0.06	3.14, 0.33	6.98, 1.30
32	A	5	1.11, 0.05	3.10, 0.32	6.96, 1.52
32	A	10	1.05, 0.05	2.99, 0.30	7.55, 2.19
32	A	15	1.00, 0.05	2.94, 0.29	7.51, 2.38
32	B	5	0.91, 0.04	2.81, 0.29	7.37, 3.24
32	C	5	0.86, 0.04	2.77, 0.28	7.29, 1.72
32	B	10	0.50, 0.02	2.34, 0.22	5.36, 0.36
32	B	15	0.134, 0.0034	1.94, 0.168	4.95, 0.38
32	B	18	0.059, 0.0010	1.85, 0.156	4.86, 0.24
Obs[a]			0.22	1.58	3.83

[a]Observed (Refs. 4 and 8) resonance positions only.

any Feshbach resonances, we performed a series of CC calculations with correlated target wave functions. These CC calculations all used CAS-CI targets in which the lowest 44 "core" electrons were frozen and the 14 active electrons were distributed between 2 a' orbitals and 8 a'' ones. The target wave functions can be represented as $(1a'-22a')^{44}(23a'24a'1a''-8a'')^{14}$ or more simply as $(\text{core})^{44}(\text{CAS})^{14}$. Starting from this target wave function it is possible to construct a number of increasingly complicated models. The simplest has L^2 configurations which can be written as

$$(\text{core})^{44}(\text{CAS})^{15},$$

$$(\text{core})^{44}(\text{CAS})^{14}(\text{virtual})^{1},$$

where the first set of configurations can be thought of representing Feshbach resonances and the second as shape resonances. It has been common but by no means a uniform[47] practice to contract the second set of CSFs with the target CI wave function(s) (Refs. 30 and 40) so that the occupation of each virtual orbital of the appropriate symmetry only contributes one (generalized) CSF no matter how large the target CI expansion is. See Ref. 40 for details. This model, which we call model A, minimizes extra correlation of the target wave function in the scattering calculation but is probably too restrictive to recover all polarization effects. Tests with and without this contraction, called model B, were performed.

Even with the uncontracted version of this model, the equivalent configurations to the two-particle-one-hole states of the SEP model are not included in the CC wave function. To allow for these in the model a further set of CSFs needs to be included. Because of the very large number of extra CSFs generated with this model it was necessary to restrict the number of active electrons. The extra L^2 configurations can be written as

$$(\text{core})^{50}(\text{CAS})^{7}(\text{virtual})^{2},$$

where the $(1a''2a''3a'')^6$ orbitals and electrons have been transferred to the core. The use of this model, denoted as C, carries the significant danger of correlating the target wave functions[30] since the CSFs can be thought of as double excitations from the CAS with the scattering electron entering the CAS.

While the calculations with model A are computationally modest, the largest reported here had 4672 CSFs for the $^2A''$ scattering symmetry and took about 20 min on a 64-bit workstation, calculations with models B and C grow rapidly. For these models we used the molecular partitioned R-matrix method[41] in which less than 10% of the eigenvalues are actually computed. The largest calculation reported here, model B with 18 virtual orbitals, gives 218 064 CSFs and took almost 3 weeks on a 64-bit workstation when the lowest 5000 energies and associated wave functions were required.

CC calculations were performed for R-matrix radii of both 10 and $13a_0$ and with both 6-31G and cc-pVDZ target basis sets. However all these calculations gave similar results and Table V only reports results for $a=13a_0$ and the cc-pVDZ target basis set. The parameters considered are the number of states included in the CC expansion, which were selected in energy order; the model used and the number of virtual orbitals available. It should be noted that the presence of many excited states in the calculation considerably complicates the resonance fitting and that fits for resonance 3 in particular proved to be trickier. In some cases, notably for the last three models reported in Table V, it proved necessary to relax the resonance criteria to allow for cases where the eigenphase increased by less than 1 rad on passing through a possible resonance. Such behavior has been encountered before in multichannel problems[48] and is a consequence of both dealing with a large number of background eigenphases and many channel thresholds. These problems can sometimes be mitigated by using alternative resonance fitting methods[49] but this was not attempted as part of this study.

The calculations reported in Table V appear to be converging with respect to the number of states included in the CC expansion; however this is an issue which we will return to in the conclusions. The change from model A to B, i.e., not contracting the CSFs of the $(\text{core})^{44}(\text{CAS})^{14}(\text{virtual})^{1}$

Downloaded 30 Apr 2009 to 128.40.5.98. Redistribution subject to AIP license or copyright; see http://jcp.aip.org/jcp/copyright.jsp

TABLE VI. Predicted resonance positions and widths in eV of $^2A'$ and $^2A''$ symmetries calculated using the cc-pVDZ target basis set, a 32 state CC calculation with model B, and 15 virtual orbitals of each symmetry. See text for further details.

Symmetry	Resonance 1	Resonance 2	Resonance 3
$^2A'$	6.17, 0.15	7.62, 0.11	8.12, 0.14
$^2A''$	0.134, 0.0034	1.94, 0.168	4.95, 0.38

type, gives a significant lowering of the resonance positions and widths. These parameters appear to change less with model C, which places two electrons in the virtual orbitals. Given the rapid increase in the size of model C calculations as the number of virtual orbitals is increased and concerns over balance between scattering and target calculations with this model, it was not pursued.

As in the SEP calculations, increasing the number of virtual orbitals within model B leads to a systematic lowering and narrowing of the resonances. Again it is not obvious that this process is actually convergent; however our model using 32 target states, 15 virtual orbitals of each symmetry and model B appears to give satisfactory results, that is they are reasonably near the observations. This model is used for our final results presented in all the following sections. We return to the issue of stability of our various models in the conclusions.

IV. RESULTS AND DISCUSSION

A. Resonances

The analysis of resonances in the previous section was conducted for $^2A''$ symmetry, which shows the presence of precisely three low-lying shape resonances. This is in agreement with most[4,24,50] but not all[15,19] previous studies. From previous studies[15,18] it is much less clear whether uracil also displays resonances of $^2A'$ symmetry.

Our SE calculations found $^2A'$ symmetry resonance features only above 10 eV. Our SEP calculations with the TZV$(2d,p)$ basis found three resonances at about 6.7, 7.9, and 8.5 eV. All these resonances proved to be very narrow, which is a well-known property of Feshbach resonances. The 8.5 eV resonance coincides with the energy where Winstead and McKoy also found the higher of their two features, for neither of which they give widths. CC calculations also showed three resonance features, albeit for the larger calculations, at slightly lower energies than those found in the SEP calculations. Parameters for these resonances are presented in Table VI, which presents our final predictions for the resonance positions and widths.

Previous studies by both Gianturco and Luchesse[15] and Winstead and McKoy[18] identified further $^2A'$ symmetry features in the 1–3 eV region. None of our calculations displayed resonancelike structures below 6 eV and we believe that these features are artifacts of the previous studies, as indeed Winstead and McKoy, in particular, suggested that they might be. The recent calculations by Gianturco *et al.*[19] found a single $^2A'$ symmetry resonance in the 8.27–8.47 eV energy range in claimed agreement with Winstead and McKoy. Our simpler SEP models predict a resonance in this region (and another one slightly higher). However these results are not stable with respect to improving the SEP calculation or, indeed, more particularly introducing a CC expansion. All our CC calculations predict three $^2A'$ resonances with the lowest in the 6 eV region.

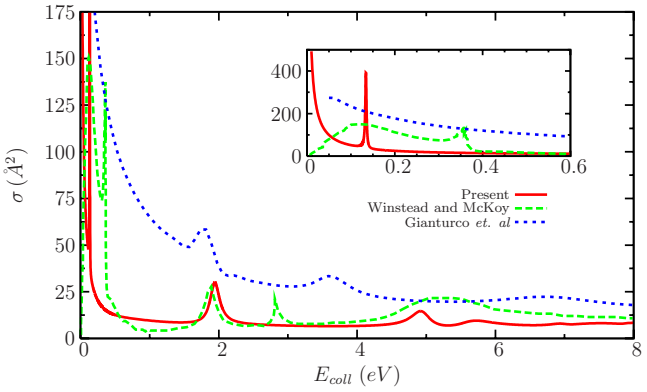

FIG. 1. (Color online) $^2A''$ symmetry contribution to the elastic cross section for low-energy electron collisions with uracil. The inset gives the low-energy behavior showing the very sharp resonance feature. Comparison is made with the calculations of Winstead and McKoy (Ref. 18) and Gianturco *et al.* (Ref. 19).

B. Cross sections

Uracil has a large dipole moment, therefore the elastic cross sections become very large at low energy. Figure 1 presents our calculated contribution due to the $^2A''$ symmetry to total elastic cross sections and compares them with those calculated by Winstead and McKoy[18] and Gianturco *et al.*[19] This cross section is quite structured due to the presence of the three low-lying shape resonances, the lowest of which can only clearly be seen in the inset. We find no evidence for the feature observed by Winstead and McKoy just below 3 eV; in addition we note that our cross section shows rapid rise at low energy as would be expected for a dipolar system.

Figure 2 gives our calculated total elastic cross section for the electron-uracil problem and compares this with previous calculations. To our knowledge there are no available comparable experimental cross sections. For our calculations that truncate the partial wave expansion of the continuum

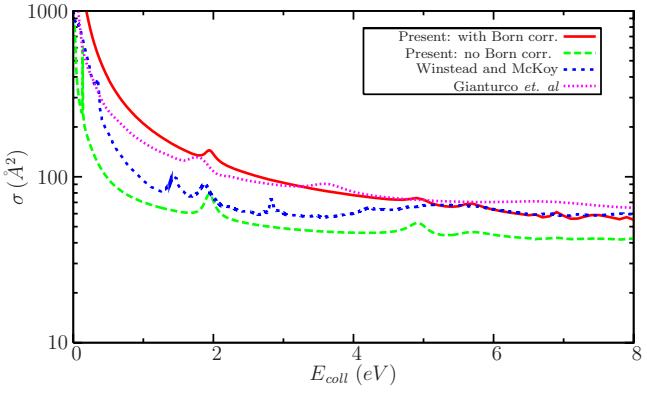

FIG. 2. (Color online) Total elastic cross section for low-energy electron collisions with uracil. Calculations with and without the Born correction are compared to the calculations of Winstead and McKoy (Ref. 18) and Gianturco *et al.* (Ref. 19).

Downloaded 30 Apr 2009 to 128.40.5.98. Redistribution subject to AIP license or copyright; see http://jcp.aip.org/jcp/copyright.jsp

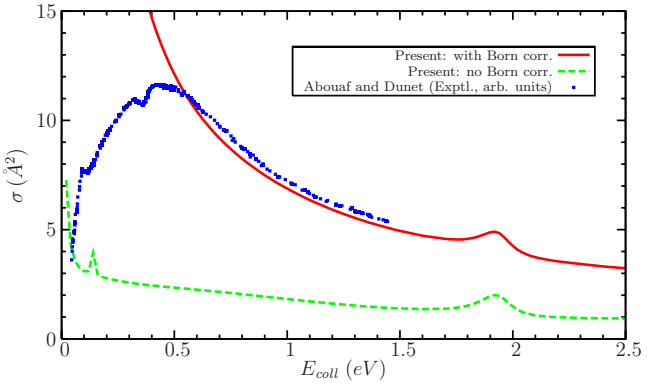

FIG. 3. (Color online) Elastic DCS at 90° for low-energy electron collisions with uracil. Calculations with and without the Born correction are compared to the nonabsolute measurements of Abouaf and Dunet (Ref. 11), which have been scaled and shifted to agree with our Born-corrected results at the higher energies.

orbitals at $l=4$, it is necessary to add a Born correction to allow for the effect of higher partial waves. This was done by adjusting the T-matrices using the "CC" cross sections generated by the code POLYDCS.[51] Some care had to be taken in choosing parameters in POLYDCS to avoid spurious structures in the differential cross section (DCS), which is a known feature of this procedure.[52] The results presented used partial waves up to $l=40$ in the Born correction and 36 Legendre polynomials in the DCS expansion.

The elastic cross section is large at all energies considered, which can be attributed to the large permanent dipole moment of the uracil target. Our calculations give reasonable agreement with the previous studies, none of which included a Born correction. However Gianturco *et al.*[19] use up to $l=80$ in their single-center expansion so it is to be expected that our Born-corrected results should be closest to these.

Although there are no reported measurements of the total elastic cross section, Abouaf and Dunet[11] measured the differential elastic cross section as a function of energy for a fixed angle of 90°. Figure 3 compares these measurements with our calculations. Since the measurements are not absolute, we have scaled and shifted them to agree with our Born-corrected results at energies above 0.5 eV. In this region it can be seen that the agreement with the energy dependence is good. At low energies the experimental DCS decreases rapidly while exhibiting features due to the low-lying shape resonances (see Fig. 1). This is contrary to all theory and to what one would expect for a strongly dipolar system.

Figure 4 presents our electron impact electronic excitation cross sections. Only excitations to the lowest four states of A' symmetry are given since all the cross sections for excitation to the A'' symmetry excited states are too small to be important; as can be seen even the A' symmetry electronic excitation cross section is fairly small. Excitation cross sections for the singlet states were augmented using a Born correction based on transition dipoles of 3.16 and 1.59 D, as calculated using MOLPRO for transitions to the $2\,^1A'$ and $3\,^1A'$ states, respectively. Above 8 eV, all our cross sections show significant structure which should be ignored as an artifact of the calculation. Winstead and McKoy,[18] who to

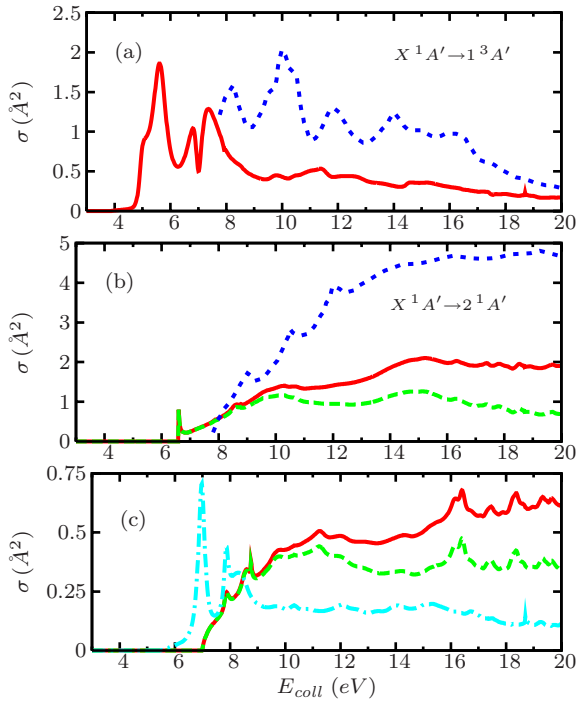

FIG. 4. (Color online) Low-energy electron impact electronic excitation cross sections for uracil in comparison to the calculations of Winstead and McKoy (Ref. 18): only excitations to the four lowest A' symmetry states are shown since the cross sections for excitation to the corresponding A'' states are very small. (a) Solid curve: present calculation, short dashed curve: Winstead and McKoy. (b) Solid curve: present calculation with Born correction, long dashed curve: present calculation without Born correction, short dashed curve: Winstead and McKoy. (c) Solid curve: present calculation for $X\,^1A' \rightarrow 3\,^1A'$ excitation with Born correction, long dashed curve: present calculation for $X\,^1A' \rightarrow 3\,^1A'$ excitation without Born correction, chain curve: present calculation for $X\,^1A' \rightarrow 2\,^3A'$ excitation.

our knowledge are the only other sources of these cross sections, make a similar observation. In general our excitation cross sections are similar to those of Winstead and McKoy; the main differences being the excitation to the $1\,^3A'$ state below 8 eV, where the resonances present in our CC calculation lead to a significantly enhanced cross section, and that Winstead and McKoy predict a larger cross section for excitation to the $2\,^1A'$ state presumably because their calculation has a larger transition dipole.

V. CONCLUSION

We present a series of calculations on collisions of electrons with uracil. Of particular interest in this system is the presence of the low-energy quasibound states of the compound system, as such resonances are thought to be the key initial process in the radiation damage of living systems. In agreement with previous studies on this problem, our calculations suggest that uracil supports three shape resonances below 5 eV, all of $^2A''$ symmetry. In addition we find three somewhat higher energy resonances of $^2A'$ symmetry with predominantly Feshbach character. We find no evidence for the low-lying resonance structures of this symmetry reported in some previous studies. Our calculations suggest that it is quite difficult to both characterize and obtain secure predic-

Downloaded 30 Apr 2009 to 128.40.5.98. Redistribution subject to AIP license or copyright; see http://jcp.aip.org/jcp/copyright.jsp

tions of the resonance parameters given the requirement for a good representation of polarization effects in a system with many valence electrons.

The difficulty of introducing polarization effects in collision problems is well documented.[53] Recently one of us has been involved in the development of a molecular *R*-matrix with pseudostates (RMPSs) method.[54,55] This method was primarily developed for treating electron impact ionization for which it has been found to work well.[56] However an important attribute of this method is that it gives well converged target polarizabilities and, by inference, polarization potentials.[55,57] It has been found to yield excellent results even for cases where such polarization effects are known to be largest.[57] Unfortunately performing an RMPS calculation on even a relatively simple multielectron target is extremely computationally demanding;[58] it is therefore doubtful whether a good RMPS calculation for the electron-uracil problem would be feasible at present. However this is a direction which we will explore in the future as the necessary computer power becomes available.

ACKNOWLEDGMENTS

This project was funded by the UK Engineering and Physical Sciences Research Council. L.B. and T.v.M. thank EaStChem for computational support via the EaStChem Research Computing Facility.

[1] B. Boudaïffa, P. Cloutier, D. Hunting, M. A. Huels, and L. Sanche, Science **287**, 1658 (2000).
[2] L. Sanche, Eur. Phys. J. D **35**, 367 (2005).
[3] C. Desfrançois, H. Abdoul-Carime, and J. P. Schermann, J. Chem. Phys. **104**, 7792 (1996).
[4] K. Aflatooni, G. A. Gallup, and P. D. Burrow, J. Phys. Chem. A **102**, 6205 (1998).
[5] G. Hanel, B. Stir, S. Denifl, P. Scheier, M. Probst, B. Farizon, M. Farizon, E. Illenberger, and T. D. Märk, Phys. Rev. Lett. **90**, 188104 (2003).
[6] S. Denifl, S. Ptasińska, G. Hanel, B. Stir, M. Probst, P. Scheier, and T. D. Märk, J. Chem. Phys. **120**, 6557 (2004).
[7] S. Denifl, S. Ptasińska, G. Hanel, B. Stir, P. Scheier, M. Probst, B. Farizon, M. Farizon, S. Matejcik, E. Illenberger *et al.*, Phys. Scr., T **110**, 252 (2004).
[8] A. M. Scheer, K. Aflatooni, G. A. Gallup, and P. D. Burrow, Phys. Rev. Lett. **92**, 068102 (2004).
[9] A. M. Scheer, C. Silvernail, J. A. Belot, K. Aflatooni, G. A. Gallup, and P. D. Burrow, Chem. Phys. Lett. **411**, 46 (2005).
[10] K. Aflatooni, A. M. Scheer, and P. D. Burrow, Chem. Phys. Lett. **408**, 426 (2005).
[11] R. Abouaf and H. Dunet, Eur. Phys. J. D **35**, 405 (2005).
[12] P. D. Burrow, G. A. Gallup, A. M. Scheer, S. Denifl, S. Ptasińska, T. D. Märk, and P. Scheier, J. Chem. Phys. **124**, 124310 (2006).
[13] K. Aflatooni, A. M. Scheer, and P. D. Burrow, J. Chem. Phys. **125**, 054301 (2006).
[14] P. Możejko and L. Sanche, Radiat. Environ. Biophys. **42**, 201 (2003).
[15] F. A. Gianturco and R. R. Lucchese, J. Chem. Phys. **120**, 7446 (2004).
[16] A. Grandi, F. A. Gianturco, and N. Sanna, Phys. Rev. Lett. **93**, 048103 (2004).
[17] S. Tonzani and C. H. Greene, J. Chem. Phys. **124**, 054312 (2006).
[18] C. Winstead and V. McKoy, J. Chem. Phys. **125**, 174304 (2006).
[19] F. A. Gianturco, F. Sebastianelli, R. R. Lucchese, I. Baccareli, and N. Sanna, J. Chem. Phys. **128**, 174302 (2008).
[20] J. Smets, W. J. McCarthy, and L. Adamowicz, J. Phys. Chem. **100**, 14655 (1996).
[21] X. Li, L. Sanche, and M. D. Sevilla, J. Phys. Chem. B **108**, 5472 (2004).
[22] C. Winstead and V. McKoy, Phys. Rev. Lett. **98**, 113201 (2007).
[23] C. Winstead and V. McKoy, Radiat. Phys. Chem. **77**, 1258 (2008).
[24] C. Winstead and V. McKoy, J. Chem. Phys. **129**, 077101 (2008).
[25] D. Bouchiha, J. D. Gorfinkiel, L. G. Caron, and L. Sanche, J. Phys. B **39**, 975 (2006).
[26] D. Bouchiha, Ph.D. thesis, University of Sherbrooke, 2008.
[27] C. S. Trevisan, A. E. Orel, and T. N. Rescigno, J. Phys. B **39**, L255 (2006).
[28] L. A. Morgan, J. Tennyson, and C. J. Gillan, Comput. Phys. Commun. **114**, 120 (1998).
[29] S. Tonzani, Comput. Phys. Commun. **176**, 146 (2007).
[30] J. Tennyson, J. Phys. B **29**, 6185 (1996).
[31] H. J. Werner, P. J. Knowles, R. Lindh, F. R. Manby, M. Schütz *et al.*, MOLPRO, Version 2006.1, a package of *ab initio* programs, 2006.
[32] M. W. Schmidt and M. S. Gordon, Annu. Rev. Phys. Chem. **49**, 233 (1998).
[33] A. Dreuw, ChemPhysChem **7**, 2259 (2006).
[34] W. J. Hehre, R. Ditchfield, and J. A. Pople, J. Chem. Phys. **56**, 2257 (1972).
[35] R. A. Kendall, T. H. Dunning, Jr., and R. J. Harrison, J. Chem. Phys. **96**, 6796 (1992).
[36] T. H. Dunning, Jr., J. Chem. Phys. **90**, 1007 (1989).
[37] M. W. Schmidt, K. K. Baldridge, J. A. Boatz, S. T. Elbert, M. S. Gordon, J. H. Jensen, S. Koseki, N. Matsunga, K. A. Nguyen, S. J. Su *et al.*, J. Comput. Chem. **14**, 1347 (1993).
[38] R. B. Brown, P. D. Godfrey, D. McNaughton, and A. P. Pierlot, J. Am. Chem. Soc. **110**, 2329 (1988).
[39] N. Russo, M. Toscano, and A. Grand, J. Comput. Chem. **21**, 1243 (2000).
[40] J. Tennyson, J. Phys. B **29**, 1817 (1996).
[41] J. Tennyson, J. Phys. B **37**, 1061 (2004).
[42] J. Tennyson and C. J. Noble, Comput. Phys. Commun. **33**, 421 (1984).
[43] A. Faure, J. D. Gorfinkiel, L. A. Morgan, and J. Tennyson, Comput. Phys. Commun. **144**, 224 (2002).
[44] S. Salvini, P. G. Burke, and C. J. Noble, J. Phys. B **17**, 2549 (1984).
[45] C. Winstead and V. McKoy, Phys. Rev. A **57**, 3589 (1998).
[46] T. N. Rescigno, D. A. Byrum, W. A. Isaacs, and C. W. McCurdy, Phys. Rev. A **60**, 2186 (1999).
[47] H. N. Varambhia, J. J. Munro, and J. Tennyson, Int. J. Mass. Spectrom. **271**, 1 (2008).
[48] S. E. Branchett, J. Tennyson, and L. A. Morgan, J. Phys. B **23**, 4625 (1990).
[49] D. T. Stibbe and J. Tennyson, J. Phys. B **29**, 4267 (1996).
[50] P. D. Burrow, J. Chem. Phys. **122**, 087105 (2005).
[51] N. Sanna and F. Gianturco, Comput. Phys. Commun. **114**, 142 (1998).
[52] R. Zhang, A. Faure, and J. Tennyson, "Electron and positron collisions with polar molecules: Studies with the benchmark water molecule," Phys. Scr. (submitted).
[53] T. N. Rescigno, Phys. Rev. A **50**, 1382 (1994).
[54] J. D. Gorfinkiel and J. Tennyson, J. Phys. B **37**, L343 (2004).
[55] J. D. Gorfinkiel and J. Tennyson, J. Phys. B **38**, 1607 (2005).
[56] G. Halmová and J. Tennyson, Phys. Rev. Lett. **100**, 213202 (2008).
[57] M. Tarana and J. Tennyson, J. Phys. B **41**, 205204 (2008).
[58] G. Halmová, J. D. Gorfinkiel, and J. Tennyson, J. Phys. B **41**, 155201 (2008).

Downloaded 30 Apr 2009 to 128.40.5.98. Redistribution subject to AIP license or copyright; see http://jcp.aip.org/jcp/copyright.jsp